Multiple scattering of photons by atomic hyperfine multiplets

Cord A. Müller,[1] Christian Miniatura,[2] David Wilkowski,[2] Robin Kaiser,[2] and Dominique Delande[3]
[1]*Physikalisches Institut, Universität Bayreuth, D-95440 Bayreuth, Germany*
[2]*Institut Non Linéaire de Nice Sophia Antipolis, UMR 6618 du CNRS, 1361 route des Lucioles, F-06560 Valbonne, France*
[3]*Laboratoire Kastler Brossel, Université Pierre et Marie Curie, 4 Place Jussieu, F-75005 Paris, France*
(Received 5 April 2005; published 10 November 2005)

Mesoscopic interference effects in multiple scattering of photons depend crucially on the internal structure of the scatterers. In the present paper, we develop the analytical theory of multiple photon scattering by cold atoms with arbitrary internal hyperfine multiplets. For a specific application, we calculate the enhancement factor of elastic coherent backscattering as a function of detuning from an entire hyperfine multiplet of neighboring resonances that cannot be considered isolated. Our theory permits one to understand why atoms behave differently from classical Rayleigh point-dipole scatterers, and how the classical description is recovered for larger but still microscopic objects like molecules or clusters.

DOI: 10.1103/PhysRevA.72.053405 PACS number(s): 32.80.Pj, 42.25.Dd, 03.65.Nk

I. INTRODUCTION

Atomic physics and quantum optics currently discover the fascinating field of mesoscopic physics [1]. Mesoscopic phenomena are due to interference effects that survive a disorder average in phase-coherent samples. Interference effects can be observed using both genuine quantum matter waves such as electrons or ultracold atoms and classical waves such as acoustic or electromagnetic waves [2]. Arguably, the most dramatic effect is the breakdown of diffusive transport due to strong localization, a phenomenon invoked by Anderson in the context of the metal-insulator transition [3]. Strong localization has been observed unambiguously for electrons [4] and microwaves [5] in quasi-one-dimensional systems. Yet even in dilute samples far from the dense regime where strong localization could be expected, interference effects can be measured. In optics, a rather robust interference phenomenon is the coherent backscattering (CBS) effect. Here, the constructive interference between waves counterpropagating along a given multiple scattering path enhances the average diffuse intensity reflected from an ensemble of random samples in a narrow angular range around the backscattering direction [6]. Under optimal experimental conditions allowing to apply the reciprocity theorem [7], this two-wave interference enhances the intensity exactly by a factor of 2 [8].

Quantum optical systems involving multiple scattering of photons by atoms are well adapted to study general concepts of quantum transport. Indeed, atoms are very efficient point scatterers for light because the scattering cross section close to an internal resonance is huge compared to the actual atomic size. Laser-cooling techniques permit one to prepare low temperature clouds where a negligible Doppler broadening of atomic transitions preserves the phase coherence of the propagating photons. For low enough laser intensity, photons are scattered completely elastically from closed atomic dipole transitions such that inelastic scattering and absorption are absent (see, however, Ref. [9] for saturation effects at higher field intensities). Furthermore, by injecting and detecting well-defined photon polarization states, one is capable of probing the internal spin degrees of freedom of the atomic scatterers.

The experimental observation of CBS of laser light by cold atoms [10,11] has revealed the crucial impact of the internal atomic structure onto coherent photon transport. Atomic dipole transitions with a nondegenerate ground-state scatter photons like isotropic point-dipoles (also known as Rayleigh scatterers) [12]. In general, however, photons probe dipole transitions with rather high Zeeman degeneracy due to large total angular momentum. It was shown theoretically that an average over all possible angular momentum orientations then leads to an antisymmetric component of the atomic scattering tensor which reduces the interference contrast of coherent backscattering considerably [13,14]. Indeed, in the absence of an external magnetic field, photons are scattered elastically by freely orientable atomic dipoles just like electrons propagating in a sample of magnetic impurities (spin-flip scattering), and in this case interference corrections to the diffusive transport picture are cut off very efficiently [15].

Previous analytical studies of the CBS double scattering contribution *from* an infinite atomic medium [14] as well as the case of multiple scattering *inside* an infinite medium [15] treated an arbitrary single, isolated, degenerate atomic dipole transition. This description is *a priori* accurate if the hyperfine optical resonance under consideration is sufficiently far away from neighboring transitions and if the laser detuning is sufficiently small. However, Kupriyanov and co-workers [11,16] showed that the CBS enhancement factor displays a slight asymmetry as function of the probe frequency around the resonance that can only be accounted for by including the other optical hyperfine transitions. In the framework of their purely numerical calculation, they did not give a qualitative explanation for the fact that the largest asymmetry is observed in the $h\|h$ polarization channel of preserved helicity and that the higher enhancement is found towards the blue-detuned side of the transition.

Extending our previous results, we develop in the present contribution an analytical theory for multiple photon scattering from atoms with a uniform statistical distribution over the magnetic quantum numbers inside each hyperfine level of the ground state, leaving the possibility of an arbitrary population distribution of the various hyperfine levels (for

example a thermal one). We rely on the decomposition of the scattered intensity into irreducible components with respect to the rotation group. This method has been developed some time ago in atomic physics [17,18], but only today, with the advent of laser cooling techniques, we can study subtle interference effects for the multiple coherent scattering of quasimonochromatic radiation. As an application, we calculate the CBS enhancement factor as a function of probe frequency for scattering from an infinite half-space. This choice is not meant to describe a realistic experiment but minimizes the purely geometrical effects of a finite optical thickness that varies with the scattering mean-free path. Our approach explains sign and magnitude of the asymmetry observed in Ref. [11]. Furthermore, our theory permits one to describe precisely how the effective degeneracy can be reduced by tuning far from hyperfine-structure or fine-structure multiplets. This allows us to understand how more complicated objects such as molecules or clusters, that involve more and more transitions, eventually scatter light as classical objects with an optimal interference contrast. Therefore, we are able to bridge the gap towards effective theories for mesoscopic photon physics in systems with classical scatterers [19].

In Sec. II, we develop the general theory of multiple photon scattering by hyperfine multiplets in the independent scattering approximation. In Sec. III, we discuss the transition to classical scattering properties. Section IV contains the limiting cases of purely elastic scattering and the calculation of CBS from atoms with a hyperfine multiplet of overlapping resonances. With Sec. V, we conclude the paper by indicating possible extensions of the work.

II. ANALYTICAL THEORY

A. Theoretical description

We describe the photon field for weak laser intensity by one-photon Fock states $|\boldsymbol{k}\boldsymbol{\epsilon}\rangle$ with wave vector $\boldsymbol{k}$ and transverse polarization $\boldsymbol{\epsilon}$. In units where $\hbar=c=1$, the energy or angular frequency of this state is $\omega=k$. The scattering of these one-photon states by atomic dipole transitions will be described following the lines of Refs. [14,15] while generalizing to multilevel transitions.

We consider atoms at rest which are initially prepared in an electronic ground-state with angular momentum J, but possibly in any sublevel F of the corresponding hyperfine multiplet. The probe light frequency is near-resonant with an electric dipole transition connecting the electronic ground-state J to an electronic excited state $J'=J-1,J,J+1$. We assume here that the atom fine structure is well described by an *LS*-coupling scheme (Fig. 1), where the total electronic angular momentum $\boldsymbol{J}=\boldsymbol{L}+\boldsymbol{S}$ couples to the nuclear spin $\boldsymbol{I}$, producing a hyperfine multiplet $\boldsymbol{F}=\boldsymbol{J}+\boldsymbol{I}$ with $F=|I-J|,\ldots,I+J$. The energy splitting of each hyperfine multiplet then is much smaller than the fine structure splitting. This is the typical situation in alkali atoms like Rubidium: for the D2 line ($5S_{1/2}\rightarrow 5P_{3/2}$) of the Rb^{85} isotope with nuclear spin $I=5/2$, the ground-state $J=1/2$ is split into two levels with $F=2$ and $F=3$. Similarly, the excited state $J'=3/2$ is split into $F'=1$, 2, 3, 4. In this scheme, the effect of different far off-resonance fine-structure transitions $J\rightarrow J''$ with the same hyperfine quantum numbers $F\rightarrow F'$ is neglected. Other coupling cases could be easily treated along the lines of reasoning described in the present paper. In general, several optical transitions $F\rightarrow F'=F-1,F,F+1$ between the ground-state and the excited state hyperfine multiplets are allowed. We will assume that the $J\rightarrow J'$ transition is *closed* so that, after having scattered an incoming photon, the atom returns to the same ground-state hyperfine multiplet but possibly in a different hyperfine level (this is the case for the Rb D2 line).

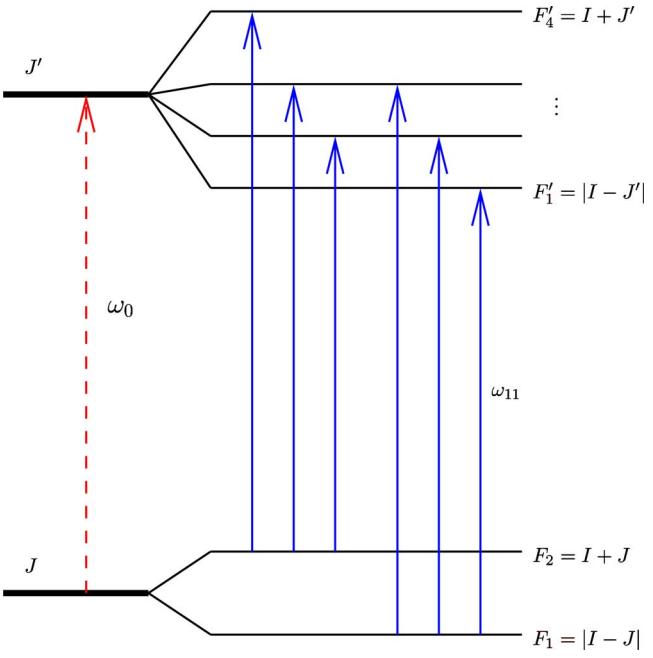

FIG. 1. (Color online) Typical level structure of an atomic dipole transition in the *LS*-coupling scheme (energy splittings not drawn to scale). First the electronic spin $\boldsymbol{S}$ ($S=1/2$ in this example) is coupled to the orbital angular momentum $\boldsymbol{L}$ (here $L=0$ in the ground state and $L=1$ in the excited state) to produce the fine structure angular momentum $\boldsymbol{J}$ (here $J=1/2$ and $J'=3/2$; $J''=1/2$ not shown). The frequency of the fine structure resonance line is ω_0 (dashed arrow). $\boldsymbol{J}$ is then coupled to the nuclear spin $\boldsymbol{I}$ to give the hyperfine angular momentum $\boldsymbol{F}$. The allowed hyperfine dipole transitions between the levels F_g and F_e' with frequencies ω_{eg} are marked with arrows.

The Hamiltonian of this internal atomic structure with ground and excited levels g and e is

$$H_{\mathrm{at}}=\sum_g \omega_g \hat{P}_g+\sum_e \omega_e' \hat{P}_e', \tag{1}$$

where ω_g is the energy of the atomic level with angular momentum F_g. $\hat{P}_g$ is the projector onto that level

$$\hat{P}_g=\sum_{m_g=-F_g}^{F_g} |F_g m_g\rangle\langle F_g m_g| \tag{2}$$

with a similar expression for the projector $\hat{P}_e'$ onto excited levels with angular momentum F_e'. Throughout the paper, the

following convention holds: primed symbols like F_e' refer to the excited state multiplet whereas unprimed symbols like F_g refer to the ground-state multiplet.

B. Scattering amplitude

While scattering a single photon $|\boldsymbol{k}\boldsymbol{\epsilon}\rangle \mapsto |\tilde{\boldsymbol{k}}\tilde{\boldsymbol{\epsilon}}\rangle$, the atom undergoes a transition $F_g \to F_f$ from an initial to a final hyperfine level. The corresponding scattering amplitude $T^{gf}(\boldsymbol{k}\boldsymbol{\epsilon} \mapsto \tilde{\boldsymbol{k}}\tilde{\boldsymbol{\epsilon}}) = \Sigma_{ij} \tilde{\boldsymbol{\epsilon}}_i^* T_{ij}^{gf}(\omega) \boldsymbol{\epsilon}_j$ is a matrix element of the scattering operator $T^{gf}(\omega)$ acting on internal atomic states and polarization vectors. According to fundamental rules of quantum theory, the amplitudes for all indistinguishable scattering processes via intermediate excited states e have to be added coherently

$$T^{gf}(\omega) = \sum_e T^{gef}(\omega). \tag{3}$$

The Cartesian components of the scattering operator for the partial scattering process $F_g \to F_e' \to F_f$ are [14]

$$T_{ij}^{gef}(\omega) = \frac{\sqrt{\omega \tilde{\omega}_{fg}}}{2\epsilon_0 V} \frac{\hat{P}_f D_i \hat{P}_e' D_j \hat{P}_g}{\omega + \omega_g - \omega_e + \mathrm{i}\,\Gamma_{eg}(\omega)/2}. \tag{4}$$

Here $\boldsymbol{D}$ is the electronic dipole operator with components D_i. Because of energy conservation the final photon frequency is $\tilde{\omega}_{fg} = \omega + \omega_g - \omega_f$. The scattering is elastic when $\tilde{\omega}_{fg} = \omega$, i.e., when the initial and final state have the same energy $\omega_g = \omega_f$. It is inelastic in all other instances.

The decay rate $\Gamma_{eg}(\omega)$ of each excited level is the sum of spontaneous decay rates to all accessible final ground-states F_f:

$$\Gamma_{eg}(\omega) = \frac{1}{3\pi\epsilon_0} \frac{1}{2F_e' + 1} \sum_f \tilde{\omega}_{fg}^3 |\langle F_e' \| \boldsymbol{D} \| F_f \rangle|^2. \tag{5}$$

For atoms used in cold atom experiments such as alkali or alkaline earth atoms, the hyperfine splitting is much smaller than ω such that the frequency difference between the various hyperfine transitions can be safely ignored for the evaluation of $\Gamma_{eg}(\omega)$, which is then a constant, the natural linewidth Γ. Note, however, that this approximation can easily be relaxed: in the formulas below describing interference effects between various hyperfine components, such as Eq. (19), one would have to use the frequency-dependent $\Gamma_{eg}(\omega)$. Since the dipole operator $\boldsymbol{D}$ acts only on the electronic angular momentum $\boldsymbol{J}$, and not on the nuclear spin $\boldsymbol{I}$, the reduced matrix element can then be reduced even further [20]:

$$\langle (J'I)F' \| \boldsymbol{D} \| (JI)F \rangle = (-)^{J'+I+F+1} \sqrt{(2F+1)(2F'+1)} \times \begin{Bmatrix} J' & F' & I \\ F & J & 1 \end{Bmatrix} \langle J' \| \boldsymbol{D} \| J \rangle. \tag{6}$$

The $6j$ symbol describes the recoupling of the four angular momenta I, J, F, and 1 for the vector operator $\boldsymbol{D}$. The sum over the final hyperfine levels F_f in (5) then can be done using a $6j$-symbol normalization rule such that one finds a uniform width for all excited hyperfine levels

$$\Gamma = \frac{\omega_0^3 d^2}{3\pi\epsilon_0}. \tag{7}$$

Here, we introduce the reduced fine structure matrix element $d = \langle J' \| \boldsymbol{D} \| J \rangle | / \sqrt{2J'+1}$. For further use, we define the dimensionless dipole operator $\boldsymbol{d}_{eg} = \hat{P}_e' \boldsymbol{D} \hat{P}_g / d$ between the levels F_e and F_g with detuning

$$\delta_{eg} = \omega + \omega_g - \omega_e. \tag{8}$$

Finally, the scattering operator takes the form

$$T_{ij}^{gef}(\omega) = \frac{3}{2\pi\rho(\omega)} \frac{\Gamma/2}{\delta_{eg} + \mathrm{i}\,\Gamma/2} (\boldsymbol{d}_{fe})_i (\boldsymbol{d}_{eg})_j. \tag{9}$$

The prefactor contains the free photon spectral density $\rho(\omega) = V\omega^2/2\pi^2$ for a given polarization in a quantization volume V.

C. Averaging over atomic degrees of freedom

Multiple scattering in the dilute regime can be depicted as a succession of scattering events by single atoms connected by propagation in an effective medium. An effective photon transport theory is obtained by a configuration average over atomic degrees of freedom. The atoms are assumed to be initially prepared independently in the ground-state levels F_g with probabilities p_g. These probabilities can represent an equilibrium distribution at a certain temperature or situations where hyperfine pumping has been achieved. Inside each level, we assume a uniform statistical distribution over magnetic quantum numbers m_g. Accordingly, the one-atom density matrix of internal degrees of freedom reads

$$\hat{\rho}_{\mathrm{at}} = \sum_g p_g \hat{\rho}_g^{(0)}, \quad \hat{\rho}_g^{(0)} = \frac{1}{2F_g + 1} \hat{P}_g. \tag{10}$$

The assumption of a scalar $\hat{\rho}_g^{(0)}$ is reasonable for optically thick samples, where the isotropization by multiply scattered photons dominates possible optical pumping effects due to the incident laser. Needless to say, this assumption greatly simplifies the calculation. In essence, an entirely analytical description is only manageable because the average over an isotropic distribution like (10) restores rotational invariance.

D. Scattering mean free path and total cross section

The wave vector k of a photon with frequency ω in the dilute atomic medium is determined by the dispersion relation $k(\omega) = \omega n_{\mathrm{r}}(\omega)$ where $n_{\mathrm{r}}(\omega)$ is the refractive index. In scattering media, the refractive index has an imaginary part that reflects the fact that scattering depletes the propagating average photon field. This defines the scattering mean free path $\mathrm{Im}k(\omega) = 1/2\ell(\omega)$. Technically, the scattering mean free path is calculated via the photon self-energy, which in turn is

proportional to the scattering operator (3) averaged over the atomic density matrix (10) [14,15]. Carrying out the isotropic sum over m_g, one finds

$$\frac{1}{\ell(\omega)} = \frac{2\pi n}{k^2}(2J'+1)\sum_g p_g \sum_e \frac{(2F'_e+1)C_{eg}^2}{1+4\delta_{eg}^2/\Gamma^2}. \tag{11}$$

Here, n is the number density of atoms. The sum over the ground-state levels g is due to the simple atomic distribution (10). The sum over the excited levels e is due to the linear superposition of scattering amplitudes, and the Lorentzian frequency dependence comes from taking the imaginary part of the resonant denominators in (3). The atomic level structure enters via the coefficients C_{eg}, a short-hand notation for the $6j$ symbols

$$C_{eg} = \begin{Bmatrix} J' & F'_e & I \\ F_g & J & 1 \end{Bmatrix} \tag{12}$$

that stem from the decomposition (6). Thanks to the $6j$-symbol normalization, they obey the following sum rules [21]:

$$\sum_e (2F'_e+1)C_{eg}^2 = \frac{1}{2J+1}, \tag{13a}$$

$$\sum_g (2F_g+1)C_{eg}^2 = \frac{1}{2J'+1}. \tag{13b}$$

Energy conservation dictates that extinction of the forward propagating mode is related to the total scattering cross section $\sigma(\omega)$ by the relation $\ell(\omega)^{-1}=n\sigma(\omega)$. This relation, the optical theorem in a multiple scattering disguise, will be proved in the following subsection. We can use it here to write the total scattering cross section as

$$\sigma(\omega) = \frac{2\pi}{k^2}(2J'+1)\sum_g p_g \sum_e \frac{(2F'_e+1)C_{eg}^2}{1+4\delta_{eg}^2/\Gamma^2}. \tag{14}$$

This total cross section is a weighted sum of Lorentzians of uniform width for all possible transitions ($g \to e \to f$). Note that this result pertains to scattering from a single hyperfine multiplet in both the ground and the excited states, i.e., a single fine-structure transition $J \to J'$. Moreover, we consider a single dipole transition with a single principal quantum number in the excited state such that no interference effects between different fine-structure transitions or different dipole transitions with the same angular momentum (as considered in Ref. [22]) can appear in the total cross section.

Since the total cross section measures the total depletion of the initial photon state, it includes both elastic scattering events where the final atomic level f is identical to the initial level g, but also inelastic scattering where the internal energy of the atom is changed. A separate evaluation of elastic and inelastic scattering is possible by considering the differential cross section.

E. Differential cross section

In the weak scattering approximation, the building block of multiple scattering is the average differential cross section for scattering polarized photons $|\boldsymbol{k}\boldsymbol{\epsilon}\rangle \mapsto |\tilde{\boldsymbol{k}}\tilde{\boldsymbol{\epsilon}}\rangle$ while the atom undergoes a transition ($g \to f$). The differential cross section is obtained by averaging the square of the scattering operator (3) over the atomic density matrix (10), giving the well-known Kramers-Heisenberg formula [23]. When all scattering processes without final frequency analysis are considered, it can be written in the form

$$\frac{d\sigma}{d\Omega} = \frac{3\sigma(\omega)}{8\pi}\mathcal{I}(\boldsymbol{\epsilon}, \tilde{\boldsymbol{\epsilon}}^*, \tilde{\boldsymbol{\epsilon}}, \boldsymbol{\epsilon}^*; \omega). \tag{15}$$

Here, the total cross section $\sigma(\omega)$ has been factorized such that the dimensionless atomic vertex funtion $\mathcal{I}$ contains all angular information about light polarization and internal atomic structure. This vertex function has been calculated in Ref. [14] for the case of a single isolated resonance $J \to J'$ using the techniques of irreducible tensor operators. Since we still assume a *scalar* density matrix (10), the vertex function must still be the sum of all possible scalar products of its vector arguments

$$\mathcal{I}(\boldsymbol{\epsilon}, \tilde{\boldsymbol{\epsilon}}^*, \tilde{\boldsymbol{\epsilon}}, \boldsymbol{\epsilon}^*; \omega) = w_1|\tilde{\boldsymbol{\epsilon}}^* \cdot \boldsymbol{\epsilon}|^2 + w_2|\tilde{\boldsymbol{\epsilon}} \cdot \boldsymbol{\epsilon}|^2 + w_3. \tag{16}$$

As in Ref. [14], the weights are given by the combinations

$$w_1 = \frac{s_0 - s_2}{3}, \quad w_2 = \frac{s_2 - s_1}{2}, \quad w_3 = \frac{s_2 + s_1}{2} \tag{17}$$

of coefficients s_K that describe scalar ($K=0$), antisymmetric ($K=1$), and symmetric ($K=2$) scattering. For the present case of multiple resonances, these coefficients are now frequency dependent

$$s_K(\omega) = \sum_g p_g \sum_f s_K^{gf}(\omega), \tag{18}$$

where each transition $g \to f$ is described by

$$s_K^{gf}(\omega) = \frac{6\pi}{k^2\sigma(\omega)}(2J'+1)^2(2F_f+1)\left|\sum_e \frac{u_K^{egf}C_{eg}C_{ef}}{1-2i\delta_{eg}/\Gamma}\right|^2. \tag{19}$$

The structure of these expressions reflects well-known rules of quantum theory: the total transition probability is the weighted incoherent sum over initial states g with occupation probability p_g, and the incoherent sum over distinguishable final states f, but the square of the coherent sum of all indistinguishable amplitudes, here related to the intermediate excited levels e. The atomic level structure enters via the coefficients C_{eg} and C_{ef} defined in (12). The essential information about the irreducible tensor modes $K=0,1,2$ of the scattering operator is contained in the factors

$$u_K^{egf} = (-1)^{F_g - F'_e}(2F'_e+1)\begin{Bmatrix} 1 & 1 & K \\ F_f & F_g & F'_e \end{Bmatrix}. \tag{20}$$

The coefficients $s_K^{gf}(\omega)$, together with the scattering mean free path (11), are the basic ingredients for computing multiple scattering quantities. The derivation of expressions (18)–(20) constitutes the main achievement of the present work. From this point on, we will essentially explore its consequences.

The total cross section (14) can be calculated from (15) by a sum over all final photon polarization vectors $\tilde{\boldsymbol{\epsilon}}$ and an angular integration over the scattered photon's direction $\tilde{\boldsymbol{k}}/|\tilde{\boldsymbol{k}}|$. This operation on the vertex function (16) yields $(8\pi/3)\times(w_1+w_2+3w_3)$. The weights (17) have been defined such that they obey the sum rule [15]

$$w_1(\omega)+w_2(\omega)+3w_3(\omega)=1, \tag{21}$$

which is equivalent to

$$\sum_{K=0,1,2}(2K+1)s_K(\omega)=3. \tag{22}$$

This last relation can be deduced from (18) by virtue of $6j$-symbol orthogonality [21] and the sum rule (13b). In a more general setting, this relation is shown to be a trace-conservation property of the intensity scattering vertex [24]. With this, we indeed recover the total cross section (14) and thus prove the optical theorem $\ell(\omega)=1/n\sigma(\omega)$ that was used above to derive the total scattering cross section directly from the mean free path.

Note that the interference between scattering amplitudes via different excited states e, present in (18), disappears in the total cross section (14). This is a result of the complete statistical average over the degenerate ground state. On the elementary level of Clebsch-Gordan coefficients, the somewhat abstract $6j$-symbol orthogonality appears as a complete cancellation of interference terms from equiprobable ground-states for large detuning.

F. Elastic versus inelastic scattering

Expression (18) of the differential cross section coefficients permits to distinguish between elastic scattering events with $f=g$ and inelastic scattering events with $f\neq g$ such that we are able to write

$$\frac{d\sigma}{d\Omega}=\sum_g p_g\sum_f\left(\frac{d\sigma}{d\Omega}\right)_{gf}, \tag{23}$$

where each transition $g\to f$ is described by its coefficients $s_K^{gf}(\omega)$ defined in (19). By integrating over final polarization and scattering directions, we can therefore write

$$\sigma(\omega)=\sigma_{\mathrm{el}}(\omega)+\sigma_{\mathrm{inel}}(\omega)=\sum_g p_g\sum_{f,e}\sigma_{gef}(\omega) \tag{24}$$

with the total cross section for each elementary transition $g\to e\to f$,

$$\sigma_{gef}(\omega)=\frac{2\pi}{k^2}(2J'+1)^2(2F_f+1)\frac{(2F'_e+1)C_{eg}^2C_{ef}^2}{1+4\delta_{eg}^2/\Gamma^2}. \tag{25}$$

By separating elastic from inelastic contributions, we therefore find $\sigma(\omega)=\sigma_{\mathrm{el}}(\omega)+\sigma_{\mathrm{inel}}(\omega)$ with

$$\sigma_{\mathrm{el}}(\omega)=\sum_g p_g\sum_e\sigma_{geg}(\omega), \tag{26}$$

$$\sigma_{\mathrm{inel}}(\omega)=\sum_g p_g\sum_{f\neq g,e}\sigma_{gef}(\omega). \tag{27}$$

In principle, a frequency analysis of the scattered photons makes it possible to measure elastic and inelastic contributions independently. Note, however, that all elastic components from the various initial states g are at the same frequency and cannot be distinguished by a frequency analysis.

Elastic scattering is of course desirable for coherent multiple scattering since the scattered photons stay on resonance. Therefore, previous experiments of coherent backscattering from degenerate atomic dipole transitions have been performed on various isolated hyperfine transitions $F\to F'$ that are closed (see Ref. [25] for a comprehensive list). Or rather, these transitions are very nearly closed: a small rate of inelastic scattering persists because after excitation to an off-resonant hyperfine level, inelastic transitions are possible. For example, the process $F_g=3\to F'_e=3\to F_f=2$ is the case of the much-studied transition $F=3\to F'=4$ of Rb^{85}. Detuning away from the closed resonance towards the other resonances, of course, increases the inelastic scattering rate. A completely consistent theory of scattering from hyperfine multiplets therefore needs to take into account inelastic scattering, without which predictions about CBS enhancement factors close to open transitions are questionable [16]. Inelastic scattering can be incorporated in Monte Carlo simulations of photon trajectories but is beyond the scope of the present article, devoted to analytical results. In Sec. IV, we will therefore specialize the interesting case where hyperfine multiplets are simultaneously excited from a unique ground state which assures purely elastic scattering.

III. TRANSITION TO CLASSICAL SCATTERING PROPERTIES

The complicated radiation pattern described by Eq. (16) is generally not the one of a classical point-dipole scatterer. But for an isotropic atomic transition $F=0\to F'=1$, there is only a single nondegenerate ground state and a single threefold degenerate excited state. In such a case, the weights coefficients in (16) are simply $w_1=1, w_2=w_3=0$, and the atom scatters light like a classical point-dipole or Rayleigh scatterer with

$$\frac{d\sigma}{d\Omega}=\frac{3\sigma(\omega)}{8\pi}|\tilde{\boldsymbol{\epsilon}}^*\cdot\boldsymbol{\epsilon}|^2,\quad \sigma(\omega)=\frac{6\pi}{k^2}\frac{1}{1+4\delta^2/\Gamma^2}. \tag{28}$$

This is equivalent to the quasiclassical model of an elastically bound electron. In this case interference effects in multiple scattering are fully preserved and the CBS enhancement factor achieves its maximal value 2 in the helicity-preserving channel [17].

In optics, scattering of light—including interference effects like CBS—by small particles (smaller than the wavelength of light) is often successfully described by modeling the small particles as classical point-dipole scatterers. However, such classical particles are very unlikely to be in a pure $F=0$ state, and we know that atoms in $F>0$ states show very low CBS interference in all polarization channels [10,13]. Therefore, the validity of the classical point-scatterer model

for complex objects with possibly many internal resonances is rather surprising. In this section, we therefore show how "classical" coherent backscattering properties are recovered for complex quantum objects (like atoms, molecules, or clusters) using a time-scale argument together with the analytical formulation developed above. In other words, we close the gap between the microscopic theory for atoms and effective models for classical scatterers.

A. Time scales

The fact that hyperfine and fine structures affect the angular distribution of the scattered light has been recognized and understood for quite some time [26]. In order to grasp how coherent light scattering depends on the hyperfine structure (or fine structure) multiplets and the detuning from resonance, it is useful to consider the various time scales coming into play.

Since F is a good quantum number, the semiclassical picture of hyperfine structure is that both the nuclear spin $\boldsymbol{I}$ and the electronic angular momentum $\boldsymbol{J}$ precess around their constant sum $\boldsymbol{F}=\boldsymbol{I}+\boldsymbol{J}$. It follows that the atomic electric dipole precesses after being excited by the incoming laser field. If the laser source is very monochromatic—linewidth smaller than the classical precession frequency, i.e., temporal coherence longer than the precession period—the radiated field is built by a coherent superposition of radiating dipoles with various spatial orientations. The net result of this coherent superposition, calculated using quantum theory of angular momenta, is the unusual radiation pattern (16). There are, however, two complications: first, the atomic dipole decays because of spontaneous emission over the time Γ^{-1}; second, if the excitation is not exactly resonant, it also oscillates at a frequency equal to the detuning δ from resonance.

These two effects are properly understood by considering the scattering of a quasimonochromatic wave packet formed by superposition of different neighboring frequencies around a central frequency ω. Such a wave packet is not scattered instantaneously, but after some delay $t_{\mathrm{W}}(\omega)$, known as the Wigner time delay. It is given by the derivative of the scattering phase shift $\arctan(2\delta/\Gamma)$—see (9)—with respect to frequency

$$t_{\mathrm{W}}(\omega)=\frac{2}{\Gamma}\frac{1}{1+4\delta^2/\Gamma^2}. \tag{29}$$

The Wigner time delay is the time scale after which the atomic dipole induced by the incoming electromagnetic field ceases to radiate coherently. It is maximum at resonance where it is twice the lifetime of the atomic excited state, and decays towards zero away from resonance.

If the Wigner time delay $t_{\mathrm{W}}(\omega)$ is longer than the period of hyperfine precession $T_\Delta=2\pi/\Delta$, where Δ is the typical hyperfine splitting, then the radiating dipole precesses during its coherence time, thus giving rise to a specific radiation pattern. This is the case at resonance if the linewidth Γ is smaller than the hyperfine splitting Δ, a situation usually encountered for an isolated hyperfine component. By contrast, if the Wigner time delay $t_{\mathrm{W}}(\omega)$ is shorter than the period of hyperfine precession T_Δ, then one expects the radiating dipole to be spatially frozen during its coherence time. Consequently, the radiation pattern should turn into the one associated with a classical dipole.

There are two obvious ways of reaching the classical scattering situation $t_{\mathrm{W}}(\omega)\ll T_\Delta$. On the one hand, if the spontaneous decay rate is larger than the hyperfine splitting, $\Gamma\gg\Delta$, the various components of the hyperfine multiplet are not resolved. The degree of freedom associated with the nuclear spin and its interaction with the electron are completely quenched on the radiative decay time scale and can be forgotten, whatever the detuning from resonance. On the other hand, when the resonances are well separated, $\Gamma\ll\Delta$, one can use large detuning to bring the Wigner time delay below the hyperfine precession period. By detuning far away from the entire multiplet of hyperfine resonances, the excitation then no longer probes the nuclear spin, and therefore scattering is only sensitive to the fine structure.

B. Analytical derivation

The full analytical theory developed in Sec. II permits one to follow precisely how the different resonance contributions combine to yield classical scattering characteristics for large detuning. When the Wigner time delay is shorter than the hyperfine period, all resonant denominators $(\delta_{eg}+\mathrm{i}\,\Gamma/2)$ can be taken equal to a common value $(\delta+\mathrm{i}\,\Gamma/2)$ where $\delta=\omega-\omega_0$ is now the detuning from the fine-structure resonance line $J\to J'$ (cf. Fig. 1). In expression (14), the resonant denominator can thus be factorized from the sum over excited states e. The sum rule (13a) together with the normalization $\Sigma_g p_g=1$ can then be used to obtain the effective fine-structure cross section

$$\sigma(\omega)=\frac{6\pi}{k^2}\frac{M_{JJ'}}{1+4\delta^2/\Gamma^2}, \tag{30}$$

where

$$M_{JJ'}=\frac{2J'+1}{3(2J+1)} \tag{31}$$

is the ratio of multiplicities normalized to $M_{01}=1$. The cross section is now independent of the hyperfine structure, i.e., no longer depend on the nuclear spin I and the population p_g of the various hyperfine levels. Similar arguments apply to the scattering of broadband radiation by thermal atoms (see especially Sec. 3.4.2. of Ref. [17]).

The radiation pattern of the scattered photons is subject to the same transformation: the frequency-dependent denominator can be factorized from the sum over e in (18). For large enough detuning, the atomic medium makes no difference between photons scattered elastically or inelastically, such that all contributions of final states f must be added. The resulting sum involves the product of three $6j$ coefficients which can be computed using the Biedenharn-Elliott sum rule [21] and everything boils down to the coefficients calculated in Ref. [14]:

$$s_K = 3(2J'+1)\begin{Bmatrix} 1 & 1 & K \\ J & J & J' \end{Bmatrix}^2. \quad (32)$$

The differential cross section then is still given by (15), its only frequency dependence being the single Lorentzian resonance of the total cross section (30).

The very same arguments apply to the electron spin responsible for the atomic fine structure. Indeed, the coupling of the electronic orbital angular momentum $\boldsymbol{L}$ with the optically inactive electronic spin $\boldsymbol{S}$ produces the total electronic angular momentum $\boldsymbol{J}=\boldsymbol{L}+\boldsymbol{S}$. Again, when the spontaneous decay rate Γ is larger than the fine-structure splitting (meaning that the various components of the fine-structure multiplet are not resolved), or when the laser frequency is far detuned from the fine-structure multiplet such that one has to sum over all possible excited levels J', one recovers the case of a $L \to L'$ transition, where only the orbital properties (directly related to the charge density response to the laser excitation) of the electrons play a role. The formulas are simply obtained from Eqs. (30)–(32) through replacement of (J,J') by (L,L').

If the ground state of an atom is an S state with $L=0$, which can be optically excited only to a P state with $L'=1$, we find $M_{LL'}=1$ and the s_K coefficients (32) simply reduce to $s_0=3$, $s_1=s_2=0$. We are back to the situation (28) where the atom radiates exactly like a classical point-dipole scatterer since only a single atomic transition $0 \to 1$ is optically active.

C. Molecules and complex objects

The previous analysis can be extended to objects slightly more complex than atoms, but whose energy spectrum and eigenstates can still be calculated. Let us for example consider a diatomic molecule with rovibrational structure. If the molecular linewidths are sufficiently small for the rotational structure to be resolved, and if the incoming light is sufficiently monochromatic for a single rotational line to be resonant, then the molecule will scatter light with the specific radiation pattern of the resonant $J \to J'$ transition. This is because the Wigner time delay is longer than the rotational period of the molecule. In contrast, if several $J \to J'=J$, $J\pm 1$ rotational transitions have to be taken into account coherently, a sum over excited states has to be performed, very similar to the one in (3), with the only difference that the dipole matrix elements depend now on the molecular quantum numbers, instead of J and F. These dipole elements are given in Ref. [27] for various possible couplings. A full discussion is beyond the scope of this paper, but the net result is as expected: the sum simplifies thanks to sum rules over $3j$ and $6j$ symbols and the radiation pattern depends only on the electronic dipole transition considered. In the most common case where it is a $\Sigma \to \Pi$ transition (the molecular equivalent of an atomic $S \to P$ transition), one recovers again as a net result the fact that the molecule scatters light like a Rayleigh scatterer.

However, when several electronic states have to be taken into account—either in atoms or in molecules—interference between several transitions is in principle still present. When one considers larger objects, such as polyatomic molecules for example, the time scales are considerably affected. The total moment of inertia increases, making the rotation slower and the corresponding classical rotation time longer. At the same time, excitations of the object decay faster, making the Wigner time delay shorter. Rotational degrees of freedom are thus quenched. Whenever the internal evolution time is longer than the Wigner time delay, one expects the internal structure to be frozen and irrelevant for light scattering properties. Generically, the shortest internal time scale which remains shorter than the Wigner time delay, will be associated with the electronic excitation, which is the degree of freedom excited in the optical frequency range. An object with more than few atoms will thus scatter "classically," i.e., following the average electronic polarizability [28]. For an object much smaller than the light wavelength (such as a cluster with, say, 1000 atoms), the multipolar expansion of the electronic polarizability will be dominated by the dipolar term, producing the dipole radiation pattern (28). There may of course be cases where the dipole contribution vanishes and higher orders dominate the radiation pattern, but such situations are certainly not generic. Finally, for objects larger than the light wavelength, the shape of the object is resolved and determines the light scattering properties. When the scatterers are anisotropic and possibly oriented, for example nematic liquid crystals in external fields, the scattering properties remain anisotropic and are described by a classical anisotropic polarizability tensor [29].

IV. ELASTIC SCATTERING

The general expressions of Sec. II simplify considerably in the case of a unique ground state since only elastic scattering can occur. This is the case when there is no hyperfine splitting (because either $I=0$ or $J=0$), or when a closed dipole transition far from other resonances is probed (cf. Fig. 2). In such cases, the $6j$ coefficients (12) obey certain selection rules and are most easily calculated using the sum rule Eq. (13b) that reduces to a single term for the only ground level F_g:

$$C_{eg}^2 = \frac{1}{(2J'+1)(2F_g+1)}, \quad (33)$$

an expression which is notably independent of the excited state(s) e. In the following, we distinguish between cases where a single excited state is relevant (and we are back to the previous results [14] and the situation where several excited states have to be considered.

A. Unique excited state

In the two situations shown in Figs. 2(a) and 2(b), there is only a single effective two-level system to be considered. In these two cases, sums over ground and excited states reduce to a single term and we recover the results of Ref. [14].

(*i*) Zero nuclear spin $I=0$. In this case, there is no hyperfine splitting and $F_g=J, F_e'=J'$. The coupling coefficient (33) is $C_{eg}^2=1/(2J+1)(2J'+1)$. The net effect is the same as for a large detuning from the multiplet discussed in Sec. III: we

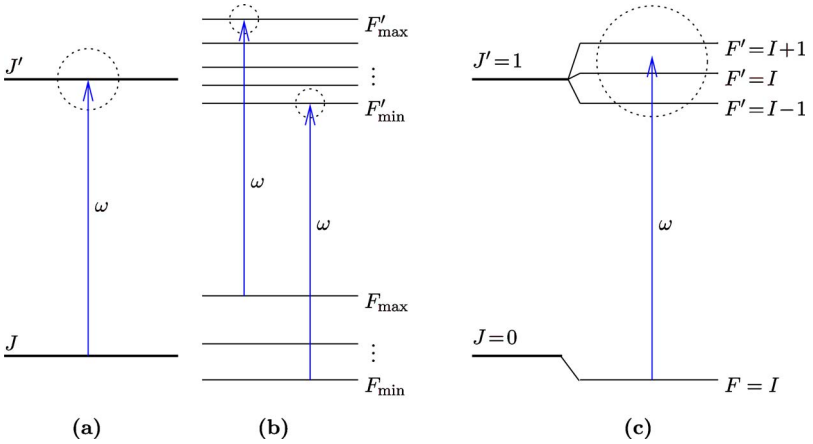

FIG. 2. (Color online) Level scheme for limiting cases of purely elastic light scattering, requiring a unique ground-state F_g. Effectively excited levels are enclosed by a dotted circle. (a) Zero nuclear spin: only the fine structure with a unique excited state is involved. (b) Resonant excitation of a closed transition $F_{\max} \to F_{\max}+1$ or $F_{\min} \to F_{\min}-1$, also with a unique excited level. (c) $J=0$: a unique ground level with $F=I$ is coherently coupled to several excited levels. Cases (a) and (b) reduce to the known results of Ref. [14]. Case (c) with a structured excited multiplet is treated analytically in Sec. IV.

recover the total cross-section (30) and the intensity vertex coefficients (32) for a $J \to J'$ transition.

(*ii*) On-resonant excitation of a *closed* transition $F_{\max}=I+J \to F'_{\max}=F_{\max}+1$ or $F_{\min}=|I-J| \to F'_{\min}=F_{\min}-1$. The latter case is possible only if $|I-J| \geqslant 1$. Naturally, the hyperfine structure splitting Δ should be large enough such that other resonances can indeed be neglected. The total cross section involves only a single term and is given by

$$\sigma(\omega) = \frac{6\pi}{k^2} \frac{M_{eg}}{1+4\delta_{eg}^2/\Gamma^2}, \tag{34}$$

with the short-hand notation

$$M_{eg} = M_{F_g F'_e} = \frac{2F'_e+1}{3(2F_g+1)} \tag{35}$$

for the ratio of multiplicities. The differential cross-section coefficients (32) are

$$s_K = 3(2F'_e+1) \begin{Bmatrix} 1 & 1 & K \\ F_g & F_g & F'_e \end{Bmatrix}^2. \tag{36}$$

These expressions are identical to Eqs. (30) and (32), with substitution of J by F_g and J' by F'_e which was the situation anticipated in Ref. [14].

B. Multiple excited states

A more interesting situation occurs when there is a unique ground state coupled to a multiplet of excited states, e.g., for a vanishing electronic ground-state angular momentum $J=0$ like in Fig. 2(c). Now the ground level $F_g=I$ is unique, and the excited level is split into the hyperfine levels $F'_e=I-1, I, I+1$ (for $I \geqslant 1$) or $F'_e=I, I+1$ (for $I=1/2$). Using Eq. (33), the total cross section (14) can be written as

$$\sigma(\omega) = \frac{6\pi}{k^2} \sum_e \frac{M_{eg}}{1+4\delta_{eg}^2/\Gamma^2}, \tag{37}$$

a sum of Lorentzians weighted by the multiplicities (35) of the various excited states. More interesting, and part of the central results of this paper, are the frequency-dependent intensity coefficients

$$s_K(\omega) = \frac{6\pi(2F_g+1)}{k^2\sigma(\omega)} \left| \sum_e \frac{u_K^{egg}}{1-2\mathrm{i}\ \delta_{eg}/\Gamma} \right|^2, \tag{38}$$

where u_K^{egg} is obtained from (20) by putting $g=f$. These coefficients permit one to describe single and multiple scattering for arbitrary detuning between and outside the resonances.

Expression (38) shows clearly that the coherent superpositon of amplitudes (3) carries through to the average intensity: the coefficients s_K are squares of interfering amplitudes and not the sum of squared amplitudes. Therefore, the influence of other resonances may lead to subtle phenomena in multiple scattering, sensitive to the differential cross section, which are not immediately visible in the total scattering cross section (37). Indeed, by virtue of a $6j$-symbol orthogonality, the total cross section is just the "incoherent" sum of the individual cross sections and therefore insensitive to these interference effects. In the classical picture, this can be nicely understood: the three hyperfine matrix elements actually originate from the same optically active transition $J=0 \to J'=1$, and the precession of $\boldsymbol{J}$ around the nuclear spin $\boldsymbol{I}$ modifies only its spatial repartition, not the total scattering rate.

In Ref. [14], elastic coherent backscattering of light by atoms has been calculated analytically in the double scattering approximation and for a semi-infinite scattering medium, at fixed detuning from an isolated resonance $J \to J'$. Now, all results of Ref. [14] can be extended to arbitrary values of light frequency. Similarly, using the Monte Carlo method described in Ref. [30], the full CBS cone (with arbitrarily large scattering orders) can be computed numerically.

As a specific example, we will consider the case of the fermionic isotope ^{87}Sr of strontium where the energy splitting between hyperfine components is comparable to the widths of the resonances themselves [31]. Figure 3(a) shows the total scattering cross section for the $^1S_0 \to {}^1P_1$ optical transition ($\Gamma/2\pi=32$ MHz) with $F_g=I=9/2$ and $F'_e=9/2, 11/2, 7/2$. The frequency separation between the $(9/2 \to 9/2)$ and the $(9/2 \to 11/2)$ resonances is 17 MHz $=0.531\ \Gamma/2\pi$ while it is 60 MHz $=1.875\ \Gamma/2\pi$ between the $(9/2 \to 9/2)$ and the $(9/2 \to 7/2)$ resonances. The vertical dotted lines indicate the position of each hyperfine resonance which clearly cannot be considered as isolated.

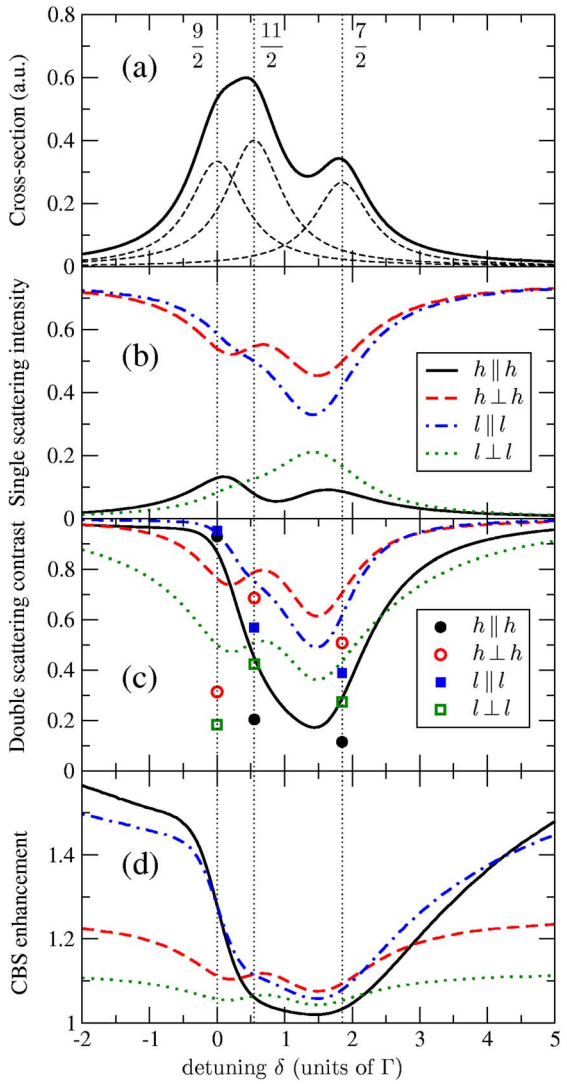

FIG. 3. (Color online) (a) Total single scattering cross section, Eq. (37), for ^{87}Sr as a function of detuning (in units of Γ). The ground-state angular momentum is $F_g=I=9/2$. There are three accessible excited states with angular momentum $F_e'=9/2,11/2,7/2$ and frequency separation $0.531\ \Gamma/2\pi$ and $1.875\ \Gamma/2\pi$ respectively. The corresponding (overlapping) optical resonances are shown by dashed lines. (b) Frequency dependence of the single scattering bistatic coefficient γ_1 for a semi-infinite medium in the four polarization channels $h\|h, h\perp h, l\|l$, and $l\perp l$. (c) Frequency dependence of the double scattering CBS interference contrast $\gamma_2^{(C)}/\gamma_2^{(L)}$ for the same situation. The predictions for isolated resonances (See Ref. [14]), indicated by the symbols, are clearly off the lines, indicating the importance of interference. (d) Frequency dependence of the total CBS enhancement factor (40). Monte Carlo calculation including all orders of scattering for a semi-infinite medium.

C. Single backscattering from a semi-infinite medium

The amount of light reflected off the sample after N scattering events can be quantified by a dimensionless parameter called the bistatic coefficient γ_N. The single scattering bistatic coefficient γ_1 in the backward direction for a semi-infinite medium with constant spatial density exposed to an incoming plane wave at normal incidence is essentially the atomic polarization vertex (16) (see Eq. (42) of Ref. [14], namely

$$\gamma_1(\omega)=\tfrac{3}{4}[w_1(\omega)|\tilde{\boldsymbol{\epsilon}}^*\cdot\boldsymbol{\epsilon}|^2+w_2(\omega)|\tilde{\boldsymbol{\epsilon}}\cdot\boldsymbol{\epsilon}|^2+w_3(\omega)]. \quad (39)$$

In Fig. 3(b), γ_1 is plotted as function of the detuning from the transition $9/2\rightarrow 9/2$ by using the frequency-dependent weights $w_i(\omega)$ given by (17) in terms of (38). The four curves correspond to the usual polarization channels: $h\|h$ (parallel helicities, i.e., opposite circular polarizations in the backward direction), $h\perp h$ (orthogonal helicities), $l\|l$ (parallel linear polarizations), and $l\perp l$ (orthogonal linear polarizations). Since we take a semi-infinite medium, every photon entering the medium must eventually exit. The atomic internal structure only redistributes photons into different polarization channels. The total intensity is independent of frequency, $\gamma_1(l\|l)+\gamma_1(l\perp l)=\gamma_1(h\|h)+\gamma_1(h\perp h)=3/4$.

Far from resonance, the atom radiates like a point-dipole scatterer, in agreement with the general discussion of the transition to quasiclassical scattering (Sec. III): since the radiated polarization is equal to the incoming one, the bistatic coefficient vanishes in the $l\perp l$ and $h\|h$ channels and takes its maximal value $3/4$ in the $l\|l$ and $h\perp h$ channels. Close to resonance, the situation is more complex. Anisotropic scattering populates all polarization channels and interference effects between the various hyperfine components are clearly made visible by the polarization analysis.

D. Double scattering interference contrast

The multiply scattered intensity ($N>1$) contains two dominant contributions: first, the so-called ladder contribution $\gamma_N^{(L)}$ without interference between multiple scattering amplitudes. This corresponds to waves copropagating along scattering paths. Second, the so-called maximally crossed contribution $\gamma_N^{(C)}$ which originates from counter-propagating waves and incorporates the interference responsible for the CBS peak. The CBS interference contrast at scattering order N is the ratio $\gamma_N^{(C)}/\gamma_N^{(L)}$. For double scattering, $N=2$, the formulas (B6) and (B24) of Ref. [14] directly give $\gamma_2^{(L)}$ and $\gamma_2^{(C)}$ at exact backscattering in terms of the weights (w_1,w_2,w_3). In Fig. 3(c), the double scattering CBS contrast $\gamma_2^{(C)}/\gamma_2^{(L)}$ is plotted as function of detuning. The on-resonant predictions for well separated resonances, shown as symbols, neglect the interference between the different resonances and are clearly not suited for quantitative predictions. Outside the multiplet, the double scattering CBS interference contrast approaches the maximum value 1 predicted for the isotropic dipole or nondegenerate transition $J=0\rightarrow J'=1$ in all channels (beyond double scattering, the contrast is unity only in the parallel channels $h\|h$ and $l\|l$), again in agreement with the general discussion in Sec. III.

Considering only the resonance with highest frequency, here $9/2\rightarrow 7/2$, it is evident that the interference contrast is generically larger towards the blue side in order to reach the optimal value 1 at large detuning. Furthermore, the largest asymmetry or slope on resonance is found for the $h\|h$ channel since it starts from the lowest contrast on resonance. These features, present in the figures of Ref. [11] but unex-

plained by the authors, therefore find a natural explanation.

E. CBS enhancement

The enhancement factor of the CBS cone is

$$\alpha = 1 + \frac{\gamma_C}{\gamma_L + \gamma_1}, \tag{40}$$

where $\gamma_L = \Sigma_{N\geqslant 2}\gamma_N^{(L)}$ and $\gamma_C = \Sigma_{N\geqslant 2}\gamma_N^{(C)}$ account for all multiple scattering orders. The presently derived weights $w_i(\omega)$ can be used for evaluating the multiply scattered intensity via the propagation eigenvalues of the ladder and crossed series, $\lambda(\omega)$ and $\chi(\omega)$, as derived in Ref. [15]. For third order scattering and beyond, exact analytic calculations become very complicated, and it is more convenient to turn to a Monte Carlo approach, as described in Refs. [30,32,33]. In Fig. 3(d), we plot the CBS enhancement factor for ^{87}Sr as a function of detuning, in the four polarization channels and for a semi-infinite medium. The most obvious observation is that the enhancement factors are typically small in the region of overlapping atomic transitions, and take larger values at large detuning, as expected from the transition to classical scattering behavior discussed in Sec. III. High orders of scattering contribute significantly to the ladder intensity, but only weakly to the CBS contribution because phase coherence is rapidly lost after the average over atomic degrees of freedom. The enhancement factor thus behaves similarly to the double scattering contrast, only amplifying the changes with the detuning.

A strong reduction of the CBS enhancement factor in the vicinity of a particular resonance may have various origins. For example, in the $h\|h$ channel, for negative detuning, the double scattering contrast is rather high. This is because the dominant contribution comes from the $9/2 \rightarrow 9/2$ transition of the $J \rightarrow J$ type with large J (see Ref. [14]). The reduction of the enhancement factor here must be attributed to single scattering. For positive detuning, the situation is opposite: single scattering is rather low, but also the double scattering contrast is poor.

In the orthogonal polarization channels $l \perp l$ and $h \perp h$, the multiple scattering CBS shows small interference contrast, because ladder and CBS contributions probe different field correlations, and thus produce a small total enhancement factor. For parallel polarization channels, $l\|l$ and $h\|h$, the enhancement factor tends to a larger value. In the $h\|h$ channel, the coherent and incoherent contributions are asymptotically equal while single scattering tends to vanish. For infinite detuning, we recover the predictions for isotropic dipole scatterers due to Ozrin [34]: 2.0 ($h\|h$), 1.25 ($h \perp h$), 1.75 ($l\|l$), 1.12 ($l \perp l$).

Note, however, that this limit is reached very slowly: the enhancement hardly exceeds 1.5 in the $h\|h$ channel for the largest detuning in Fig. 3, although it is twice as large as the total splitting Δ of the hyperfine multiplet. The reason for the slow recovery is simple to understand: for a semi-infinite medium, long scattering paths contribute significantly to the CBS cone, with all paths beyond order N giving an integrated contribution scaling like $N^{-1/2}$. At large detuning, the w_i coefficients tend to their limiting values like δ/Δ. This in turn implies that a fraction $\simeq \delta/\Delta$ of the perfect contrast is lost at each scattering event, putting an effective cutoff $\simeq \Delta/\delta$ on the scattering orders contributing to the CBS cone. Altogether, this implies that the asymptotic value 2 for the enhancement factor is reached only like $\sqrt{\delta/\Delta}$. In other words, even a small unresolved hyperfine structure may significantly reduce the interference contrast. This is a clear illustration that CBS—and any quantum interference for that matter—is very sensitive to small couplings to uncontrolled degrees of freedom.

V. CONCLUSION

In the present paper, we have considered multiple scattering of photons by a disordered medium of atom at rest with several internal resonances. We have developed the analytical calculation of the total photon scattering cross section $\sigma(\omega)$ and the differential cross section $(d\sigma/d\Omega)$ as a function of the light frequency and of the relevant angular momentum parameters defining the internal resonances. We have examined under which conditions the various resonances conspire to yield the classical model of an isotropic dipole. As an application of the theory to multiple elastic scattering from hyperfine multiplets, we have calculated the CBS enhancement for a hypothetic half-space with a homogeneous average density of atoms.

The present paper makes two major restrictive assumptions that should be lifted in subsequent investigations. First, the results presented in Sec. IV for the CBS enhancement factors have been calculated for the case of a closed transition with a unique ground state assuring purely elastic scattering. The more general case of inelastic scattering from open transitions can be treated along the same lines by using the analytical theory developed in Sec. II. Second, real experiments with cold atoms are not performed on semi-infinite homogeneous media, but on inhomogeneous clouds of finite optical thickness. Their mean free path and thus the optical thickness change drastically under detuning from resonance. This in turn modifies the relative weight of different scattering orders and therefore also the enhancement factor. Consequently, for scattering media of finite extent, these purely geometrical effects must be taken into account. An efficient numerical Monte Carlo method for this situation has been presented in Ref. [30]. The above analytical expressions for the mean free path and the intensity vertex coefficients can be introduced into this program and permit one to obtain accurate CBS enhancement factors and full peak shapes for quantitative comparison with experiments. However, both questions are beyond the scope of the present contribution and will be discussed elsewhere.

ACKNOWLEDGMENTS

Ch.M. wishes to thank J. Dupont-Roc for useful discussions. Laboratoire Kastler Brossel de l'Université Pierre et Marie Curie et de l'École Normale Supérieure is UMR 8552 du CNRS. CPU time on various computers has been provided by IDRIS. The work was supported by the PROCOPE program of MAE and DAAD.

[1] *Mesoscopic Quantum Physics*, in Proceedings of the Les Houches Summer School, Session LXI, edited by E. Akkermans and G. Montambaux and J. L. Pichard, and J. Zinn-Justin (North Holland, Elsevier Science B. V., Amsterdam, 1995).
[2] E. Akkermans and G. Montambaux, *Physique Mésoscopique des Électrons et des Photons*, (EDP Sciences, CNRS Editions, Paris 2004). An English translation is in preparation.
[3] For reviews, see P. A. Lee and T. V. Ramakrishnan, Rev. Mod. Phys. **57**, 287 (1985); B. Kramer and A. MacKinnon, Rep. Prog. Phys. **56**, 1469 (1993).
[4] Y. B. Khavin, M. E. Gershenson, and A. L. Bogdanov, Phys. Rev. B **58**, 8009 (1998).
[5] A. A. Chabanov and A. Z. Genack, Phys. Rev. Lett. **87**, 153901 (2001).
[6] M. P. van Albada and A. Lagendijk, Phys. Rev. Lett. **55**, 2692 (1985); P. E. Wolf and G. Maret, *ibid.* **55**, 2696 (1985).
[7] B. A. van Tiggelen and R. Maynard, in *Wave Propagation in Complex Media*, IMA Volumes in Mathematics and its Applications Vol. 96, edited by G. R. Papanicolaou (Springer, New York, 1998), pp. 247–271.
[8] D. S. Wiersma, M. P. van Albada, B. A. van Tiggelen, and A. Lagendijk, Phys. Rev. Lett. **74**, 4193 (1995).
[9] T. Chanelière, D. Wilkowski, Y. Bidel, R. Kaiser, and C. Miniatura, Phys. Rev. E **70**, 036602 (2004); T. Wellens, B. Grémaud, D. Delande, and C. Miniatura, Phys. Rev. A **70**, 023817 (2004); V. Shatokhin, C. A. Müller, and A. Buchleitner, Phys. Rev. Lett. **94**, 043603 (2005).
[10] G. Labeyrie, F. de Tomasi, J. C. Bernard, C. A. Müller, C. Miniatura, and R. Kaiser, Phys. Rev. Lett. **83**, 5266 (1999).
[11] D. V. Kupriyanov, I. M. Sokolov, P. Kulatunga, C. I. Sukenik, and M. D. Havey, Phys. Rev. A **67**, 013814 (2003); D. V. Kupriyanov, I. M. Sokolov, N. V. Larionov, P. Kulatunga, C. I. Sukenik, S. Balik, and M. D. Havey, *ibid.* **69**, 033801 (2004).
[12] Y. Bidel, B. Klappauf, J. C. Bernard, D. Delande, G. Labeyrie, C. Miniatura, D. Wilkowski, and R. Kaiser, Phys. Rev. Lett. **88**, 203902 (2002).
[13] T. Jonckheere, C. Müller, R. Kaiser, C. Miniatura, and D. Delande, Phys. Rev. Lett. **85**, 4269 (2000).
[14] C. A. Müller, T. Jonckheere, C. Miniatura, and D. Delande, Phys. Rev. A **64**, 053804 (2001).
[15] C. A. Müller and C. Miniatura, J. Phys. A **35**, 10163 (2002).
[16] D. V. Kupriyanov, I. M. Sokolov and M. D. Havey, Opt. Commun. **243**, 165 (2004).
[17] A. Omont, Prog. Quantum Electron. **5**, 69-138 (1977).
[18] K. Blum, *Density Matrix Theory and Applications* (Plenum Press, New York, 1996).
[19] E. Akkermans and G. Montambaux, J. Opt. Soc. Am. B **21**, 101 (2004).
[20] A. R. Edmonds, *Angular Momentum in Quantum Mechanics* (Princeton University Press, Princeton, 1960).
[21] M. Rothenberg, R. Bivins, M. Metropolis, and J. K. Wooten, *The 3-j and 6-j symbols* (Crosby Lockwood, London, 1959); D. A. Varshalovich, A. N. Moskalev and V. K. Khersonskii, *Quantum Theory of Angular Momentum* (World Scientific, Singapore, 1988).
[22] D. A. Cardimona, M. G. Raymer, and C. R. Stroud, Jr., J. Phys. B **15**, 55 (1982).
[23] R. Loudon, *The Quantum Theory of Light* (Oxford University Press, New York, 2000).
[24] C. A. Müller *et al.*, J. Phys. A **38**, 7807 (2005).
[25] D. Wilkowski *et al.*, J. Opt. Soc. Am. B **21**, 183 (2004).
[26] A. C. Tam and C. K. Au, Opt. Commun. **19**, 265 (1976); R. Walkup, A. L. Migdall and D. E. Pritchard, Phys. Rev. A **25**, 3114 (1982). For a review over results in the early days of quantum theory, see G. Placzek, in *Handbuch der Radiologie* 6 (Akademische Verlagsgesellschaft, Leipzig, 1934) Vol. 2 pp. 205-374:
[27] B. R. Judd, *Angular Momentum Theory for Diatomic Molecules* (Academic Press, New York, 1975).
[28] V. B. Berestetskii, E. M Lifshitz, and L. P. Pitaevskii, *Quantum Electrodynamics*, (Butterworth-Heinemann, Oxford, 1982), Secs. 60 and 61.
[29] B. A. van Tiggelen and H. Stark, Rev. Mod. Phys. **72**, 1017 (2000).
[30] G. Labeyrie, D. Delande, C. A. Müller, C. Miniatura, and R. Kaiser, Phys. Rev. A **67**, 033814 (2003).
[31] X. Xu, T. H. Loftus, J. L. Hall, A. Gallagher, and J. Ye, J. Opt. Soc. Am. B **20**, 968 (2003).
[32] G. Labeyrie, D. Delande, C. A. Müller, C. Miniatura, and R. Kaiser, Europhys. Lett. **61**, 327 (2003).
[33] V. L. Kuzmin and I. V. Meglinski, JETP Lett. **79**, 109 (2004); K. Muinonen, Waves Random Media **14**, 365 (2004).
[34] V. D. Ozrin, Waves Random Media **2**, 141-164 (1992).